



Impacts of Satellite-Derived Leaf Area Index on North American Warm-Season Climate Variability in a Regional Atmospheric Model

Christopher L. Castro
Department of Atmospheric Sciences, University of Arizona
E-mail: castro@atmo.arizona.edu

Adriana Beltrán-Przekurat and Roger A. Pielke, Sr.
CIRES, University of Colorado at Boulder



Introduction

Our previous work has established that the dominant impacts of Pacific sea surface temperatures (SSTs) influence the summer climate of North America via remote forcing of the large-scale circulation, or teleconnections. These teleconnections evolve in time and are most apparent during the early part of the summer, affecting the onset of the North American monsoon and the end to the late spring wet period in the central U.S. It has also been established via regional climate models (RCMs) that the land surface influences of soil moisture and vegetation may significantly impact summer climate. The hypothesis posed here is that the land surface influences become more important during the latter part of the summer, when the influence of remote Pacific SST forcing diminishes. To investigate this, we first perform a statistical analysis to determine the dominant spatiotemporal variability of the precipitation (SPI) and vegetation greenness. Then RCM simulations with the Regional Atmospheric Modeling System that incorporate the satellite-derived leaf area index (LAI) are performed for the period 1982-2003 and compared to our prior simulations (reported in Castro et al. 2007, *J. Climate*) that have a fixed climatological LAI and observations. Finally, specific years with extreme warm season climate conditions, based on the spatiotemporal analysis, are selected to investigate the potential influence of vegetation via a series of model sensitivity tests. The vegetation dataset used in this study is the Global Inventory Modeling and Mapping Studies Satellite Drift Corrected and NOAA-16 incorporated Normalized Difference Vegetation Index (GIMMS-NDVI).

Spatiotemporal Analysis of SPI and Vegetation Greenness

Multitaper Method Singular Value Decomposition (MTM-SVD) allows for the detection and reconstruction of quasi-oscillatory spatio-temporal climate signals that exhibit episodes of spatially correlated behavior. It produces: 1) a local fractional variance (LFV) spectrum of the principal eigenmode; 2) statistical confidence intervals for the LFV spectrum; and 3) reconstructed anomaly patterns corresponding to the significant time-varying modes (e.g. Rajagopalan et al. 1998). This statistical analysis technique was applied to the standardized precipitation index (SPI) computed from the CPC U.S.-Mexico precipitation dataset, and to the GIMMS-NDVI, normalized using the SPI procedure. In the reconstructed pattern anomaly maps shown below, the vectors indicate the degree of phasing with respect to a grid point in the central U.S.

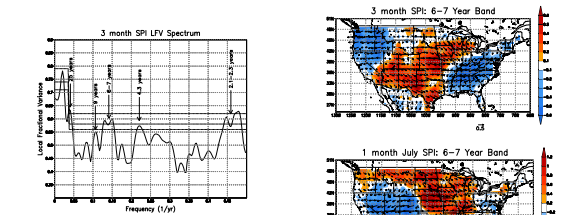


Figure 1: Principal eigenmode LFV spectrum of 3 month SPI for CPC U.S.-Mexico precipitation data (1950-2002). Dashed line indicates statistical significance at the 90% and 99% levels, respectively. Statistically significant spectral peaks indicated.

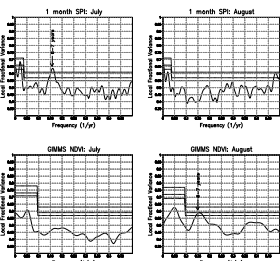


Figure 2: Same as Fig. 1 for 1 month SPI in July and August (top) and GIMMS NDVI in July and August (bottom).

Considering all months of the year, the significant time variation in 3 month SPI is shown in Fig. 1. We focus on the signal in the 6-7 year band, as significant variability in GIMMS-NDVI occurs at this same timescale. The reconstructed spatial pattern of 3 month SPI in this band (Fig. 2, top) is indicative of a wintertime ENSO-PDO precipitation response. However, considering the same signal only for the month of July with 1 month SPI (Fig. 2, bottom), the signal reflects interannual variability in North American monsoon, with precipitation variability in the central U.S. out of phase with the southwestern U.S. Significant interannual variability in the monsoon precipitation signal is present in July, but not August (Fig. 3, top). The vegetation then responds to the interannual variability in monsoon precipitation in August (Fig. 3, bottom). Differences in vegetation greenness associated with variability in the 6-7 year band are most apparent in places impacted by monsoon rainfall, such as Arizona (Fig. 4).

Satellite-Derived LAI vs. RAMS model default LAI

Several studies have shown that significant feedbacks occur on seasonal time scales when vegetation is allowed to evolve as part of the dynamic modeling system (Lu et al. 2001). Prescription in seasonal climate simulations of the vegetation phenology based on climatology can result in strong atmospheric biases in atmospheric variables and surface fluxes (i.e., Xue et al. 1996; Lu and Shuttleworth 2002). For example, modeling simulations performed with RAMS, leaf area index (LAI) is initialized based on a prescribed annual cycle for each vegetation type, based on date and latitude. Therefore, this dataset is not able to incorporate to the simulations the regional heterogeneity and interannual variability found in the observed LAI fields (e.g. as in Figures 3 and 4). Figures below show the satellite-derived LAI vs. RAMS default-LAI climatology for the warm season on the simulation domain used in Castro et al. (2007). RAMS default climatology seems to dramatically overestimate the LAI, on average, compared to the GIMMS-derived product. Here we show the differences for the year 1988, as the same difference patterns were observed for all years in the GIMMS-NDVI record.

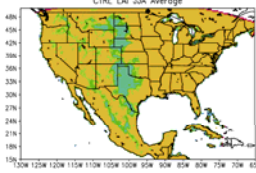


Figure 5: RAMS model default specification of warm season LAI ($m^2 m^{-2}$) within the model land surface scheme.

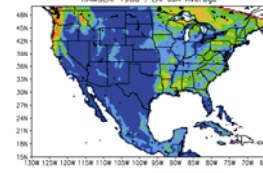


Figure 6: Same as Fig. 5 for LAI derived from GIMMS-NDVI data for 1988.

Effect of Satellite-Derived LAI on model simulation results

To study the effect of these two different LAI conditions on warm-season climate variability, RCM simulations were performed with the Regional Atmospheric Modeling System (RAMS) replacing the default-LAI climatology with daily GIMMS-NDVI LAI. Simulation experiments were performed with a similar model set-up as in Castro et al. (2007) for the period 1982-2003. These new simulations (named RAMSLAI) are compared to our prior simulations, CTRL (reported in Castro et al. 2007). Results are shown for precipitation and near-surface fluxes. Large rainfall changes can be seen throughout the simulations, in particular in areas of the western and central U.S. and central Mexico, corresponding in general to areas where LAI is very different between the model default vs. satellite derived product. The runs with the satellite-derived LAI appear to give a more realistic representation of warm season rainfall and help correct high precipitation biases noted in the original Castro et al. (2007) simulations. Differences in LAI also affect near-surface sensible (SH) and latent (LH) heat fluxes. Average June-July-August differences in SH and LH appear collocated with the largest LAI differences.

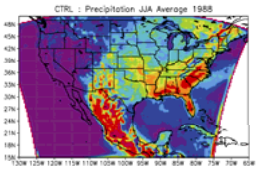


Figure 7: Model simulated monthly average warm season precipitation (mm) for the control 1988 case with the model default LAI as shown in Fig. 5.

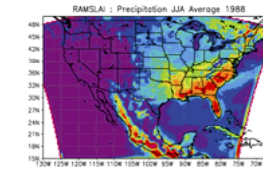


Figure 8: Model simulated monthly average warm season precipitation (mm) for the 1988 case with LAI specified from GIMMS-NDVI as shown in Fig. 6.

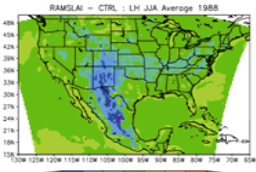


Figure 9: Difference in model simulated latent heat flux ($W m^{-2}$) for 1988 controlled with default LAI specification as shown in Fig. 5 vs. LAI specified from GIMMS-NDVI as shown in Fig. 6.

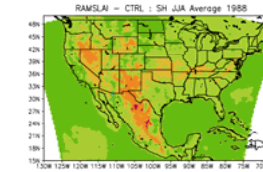


Figure 10: Same as Fig. 9 for sensible heat flux.

Swapped LAI Sensitivity Experiments for Extreme Warm Seasons

In a second set of RAMS sensitivity experiments, specific years with extreme warm season climate conditions, based on the spatiotemporal analysis of SPI and NDVI, are selected to investigate the potential influence of vegetation. The two archetypal years of 1988 and 1993 are investigated first because anomalous early warm season precipitation is tied to Pacific SST associated teleconnections and soil moisture sensitivity studies have been previously performed for these years using other regional atmospheric models. As a relatively simple test, the GIMMS-derived LAI was swapped between these two years, such that 1993 LAI was used with 1988 atmospheric boundary conditions and vice versa. The LAI differences and model simulated precipitation (for actual LAI vs. LAI swapped simulations) are shown below. Results are shown for early and late summer, as the late period is the time when Pacific SST associated teleconnections diminish. For both 1988 and 1993 sets of model simulations, 1) precipitation differences are highly localized and less than the spatial scale of the LAI differences; 2) in the central U.S., increases in precipitation appear to be associated with lower LAI and, thus, higher sensible heat fluxes; 3) greater precipitation differences occur in the year where there was more atmospheric moisture from remote sources (1993).

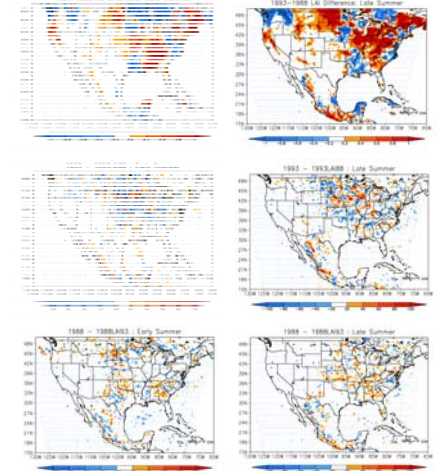


Figure 11: Differences in 1993 and 1988 RAMS sensitivity simulations, for early summer (June through early July) and late summer (late July through August). Top: difference in GIMMS-NDVI derived LAI ($m^2 m^{-2}$). Middle: differences in precipitation (mm) for 1993 simulations. Bottom: differences in precipitation for 1988 simulations.

Additional sensitivity experiments were performed for 1984, a year with a very wet and early North American monsoon that caused relatively high vegetation greenness during the latter part of the summer in northwest Mexico. NDVI for 1984 projects negatively on the spatial pattern in Fig. 4. For the swapped LAI, the year 1993 is used as the monsoon was very dry and delayed. Results are very similar to the 1988 and 1994 simulations in that precipitation differences are highly localized and are greater during the period of heavier precipitation, late summer in the case of the core monsoon region.

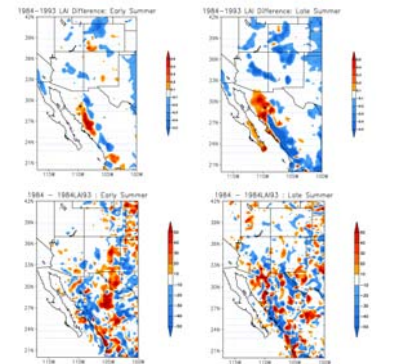


Figure 12: Same as Fig. 11 for 1984 sensitivity experiments for the core North American monsoon region. Note that the scale has been reduced for LAI and precipitation differences.